

# Preparation of self-lubricating porous alumina ceramics with PMMA /PAO6 microcapsules and their tribological properties

Ziqi Cheng<sup>a</sup>, Hanjun Gong<sup>b</sup>, Zheng Wang<sup>a</sup>, Lina Zhu<sup>a,c,\*</sup>, Guoxin Xie<sup>b,\*\*</sup>

<sup>a</sup> School of Engineering and Technology, China University of Geosciences, Beijing, 100083, China

<sup>b</sup> State Key Laboratory of Tribology, Tsinghua University, Beijing, 100084, China

<sup>c</sup> Zhengzhou Institute, China University of Geosciences Beijing, Zhengzhou, 451283, PR China

## ARTICLE INFO

### Keywords:

- B. composites
- C. Friction
- D. Wear resistance
- D. Al<sub>2</sub>O<sub>3</sub>

## ABSTRACT

In this work, we showed that immersing polymethyl methacrylate (PMMA)/poly alpha olefins (PAO6) microcapsules into the porous matrix can improve the lubrication properties of porous alumina ceramics dramatically. PMMA/PAO6 microcapsules were synthesized by microemulsion polymerization, and the microcapsules were immersed in the porous alumina ceramic matrix by vacuum impregnation. The lubrication behaviors of the porous alumina ceramics with PMMA/PAO6 microcapsules have been investigated under different loads. As compared with the unprocessed porous alumina ceramics, the coefficient of friction (COF) of the porous ceramics impregnated with microcapsules could be reduced to 4% of that without microcapsules, and the wear rate could be reduced by two orders of magnitude. No obvious change of the COF was noticed for the matrices with different pore sizes. The good self-lubrication properties were achieved by releasing the PAO6 in the microcapsules during the friction process.

## 1. Introduction

Ceramic materials have excellent mechanical properties and good oxidation resistance, which provides a wide range of applications in mechanics, aerospace [1,2], marine biological engineering [3], etc. As a type of ceramic material, porous ceramics have the advantages of lightweight and high strength. However, under dry sliding conditions, the coefficient of friction (COF) of ceramics is relatively high (usually 0.4–0.8) [4–7]. There were many drawbacks when liquid lubricants were used under specific working conditions. Owing to the benefits of porous ceramics, many studies had been conducted on improving the lubrication performance of porous ceramics. These researches include adding oil or melted solid lubricants [8] to porous ceramics by impregnation, synthesizing solid lubricants on the surface of the porous ceramic matrix [9], and filling the second phase solid lubricants, such as graphite [10], hexagonal boron nitride (*h*-BN) [11], carbon fiber [12], into the porous ceramic matrix.

The addition of oil into the ceramics was a simple way to improve the lubrication performance of the ceramic. There were a variety of similar methods that could improve the lubrication of porous ceramics. On the basis of a study conducted by Sang et al. [8] in which molten Ni and

fluoride were immersed into porous ceramics, the COF and the wear rate did not improve and the COF even began to increase when the temperature was below 300 °C. The self-lubricating properties of the composite ceramics have been characterized only when the temperature was above 600 °C. The method of synthesizing solid lubricants in porous ceramics used by Abdul et al. [9] could obtain self-lubricating performance of porous alumina ceramics at room temperature. Nevertheless, it was a tedious process, and in many cases the penetration of solid lubricants in the ceramic matrix was insufficient. Another common method of adding the secondary phase of solid lubricant into the ceramic matrix could also play a part in the improvement of lubrication. However, this method suffered from the fact that most of the lubrication properties were only improved merely under specific conditions. The COF and the wear rate would even increase under the dry friction condition [13,14]. It was now well established from the above researches that adding lubricating polymers into the ceramic matrix could improve the lubricating properties of porous ceramics. Therefore, it is necessary to develop composites that can easily penetrate into the porous ceramic matrix while maintaining good lubricating properties.

In recent years, core-shell composites have attracted extensive attention [15–20]. They were normally composed of two or more

\* Corresponding author. School of Engineering and Technology, China University of Geosciences, Beijing, 100083, China.

\*\* Corresponding author.

E-mail addresses: [zhulina@cugb.edu.cn](mailto:zhulina@cugb.edu.cn) (L. Zhu), [xgx2014@tsinghua.edu.cn](mailto:xgx2014@tsinghua.edu.cn) (G. Xie).

<https://doi.org/10.1016/j.ceramint.2021.12.003>

Received 30 August 2021; Received in revised form 1 November 2021; Accepted 1 December 2021

Available online 3 December 2021

0272-8842/© 2021 Elsevier Ltd and Techna Group S.r.l. All rights reserved.

different materials, and adjusting the material composition of the core-shell particles by actual design can achieve superior performance than a single material. Core-shell materials have a broad application prospect in medicine [21], sensor [22], catalysis [23] lubrication [24, 25], etc.

Microcapsule is a typical core-shell material, its shell material and core material are usually selected according to the application field. When used in the field of lubrication, many polymers such as polystyrene [26] and polymethyl methacrylate [27,28] were used as the shell materials. And its nuclear material is usually various types of lubricants.

Nanocomposites with polymer matrices encapsulating liquid lubricants have excellent mechanical and lubricating properties, which are suitable for the occasions where external lubricants are unsuitable. These polymer composites were often mixed with other matrix phases such as epoxy resin [29–33], polyurethane [34], aluminum oxide ( $\text{Al}_2\text{O}_3$ ) [35] to produce composites with enhanced mechanical and lubrication properties.

The core-shell polymer composite materials had good lubricating properties and the advantages of solid lubricating materials. Therefore, in this work, microemulsion polymerization was used to prepare microcapsules with polymethyl methacrylate (PMMA) shell filled with poly alpha olefins (PAO6) oil. The synthesized microcapsules were infiltrated into porous alumina ceramics by vacuum impregnation to obtain porous ceramics with desirable self-lubricating properties. On the basis of macroscopic frictional experiments with the ball-on-disc configuration, the lubrication performances of porous ceramics containing microcapsules were systematically examined. The results demonstrated that the porous alumina ceramics with microcapsules possessed excellent lubrication properties.

## 2. Experimental

### 2.1. Materials

Methyl methacrylate (MMA, 99%, Meryer, Shanghai, China) was passed over basic alumina prior to use. 2, 20-Azobisisobutyronitrile was purchased from Beijing J&K in China. All of the above materials were retained below. Hexadecane (HD, 98%) was supplied by Meryer (Shanghai, China). Sodium n-dodecyl sulphate (SDS 99%) was provided by National Medicine Group Chemical Reagent Co., Ltd. PAO6 was purchased from Shanghai Qi Cheng Industrial Co., Ltd. The porous ceramics were supplied by Guizhou Meirui New Material Technology Co., Ltd.

### 2.2. Synthesis of PMMA microcapsules containing PAO oil

Studies by Guo et al. [36] have shown that microcapsules of different sizes can be synthesized by changing the concentration of surfactants and co-stabilizers. Therefore, we changed the size of the microcapsules by reducing the ultrasonic speed and increasing the concentration of co-stabilizer and surfactant. Two types of PMMA-PAO6 microcapsules

with diameters of 60–70 nm and 200–400 nm were prepared through the microemulsion polymerization method. The schematic diagram was shown in Fig. 1.

Firstly, the PAO6 and HD were added into PMMA, and magnetic stirring was used to form the dispersed phase. For the preparation of the surfactant solution, SDS was added into deionized water, and the dispersed phase solution was then added. Subsequently, the mixed solution was transferred into the cell crusher for ultrasonic microemulsification. In order to avoid polymerization owing to the temperature increase during the ultrasonic process, an icy water bath was used for cooling. Afterwards, the solution was transferred into a three-necked flask filled with nitrogen for further reaction at 75 °C under agitation for about 5 h. Finally, the synthesized microcapsules solution was sealed and stored at room temperature before being impregnated to the porous alumina ceramics.

### 2.3. Preparation of the porous $\text{Al}_2\text{O}_3$ ceramics with microcapsules

The porous alumina ceramics with PMMA/PAO6 microcapsules were prepared by the vacuum impregnation method. To better penetrate the microcapsules into the deep part of the porous ceramics, multiple impregnations were carried out during the preparation process. As shown in Fig. 2, porous alumina ceramics were immersed in the solution with microcapsules of 60–70 nm in diameter, and transferred to a vacuum chamber. The solution with microcapsules was permeated into the porous matrix by using a negative pressure for more than 36 h. Subsequently, the porous alumina ceramics were baked in an oven at 45 °C for 6 h to remove the water in the solution. After the first drying, the porous alumina ceramics were once more immersed in the PMMA/PAO6 microcapsules solutions with the diameters range of 200 nm–400 nm. Then, the porous alumina ceramics were baked in an oven at 45 °C until complete drying. During the drying process, the microcapsules agglomerated, and individual microcapsules gathered together.

### 2.4. Materials characterization

The morphology of PMMA/PAO6 microcapsules was observed by scanning electron microscopy (SEM, Hitachi SU8220). The diluted solution with microcapsules was dripped onto a silicon wafer surface and a splattered Pt surface after drying. The shell thickness of the PMMA/PAO6 microcapsule was measured by transmission electron microscopy (TEM, JEM-2100F). The morphology of porous alumina ceramics was characterized by environment scanning electron microscopy (ESEM, FEI Quanta 200 FEG). X-ray diffraction (XRD, Bruker, Rint 2000) was applied to characterize the structure of the porous alumina ceramics with capsules. The three-dimensional morphology of wear marks and the wear rate were obtained by using the three-dimensional white light interference surface topography device (Zygo Nexvie).

The friction tests of porous ceramics with microcapsules were carried out by using the UMT-3 universal micro-friction and wear tester from CETR Corporation with the ball-disk configuration. The grinding balls were zirconia ( $\text{ZrO}$ ) ceramic balls,  $\phi 3.98$  mm the balls were rinsed

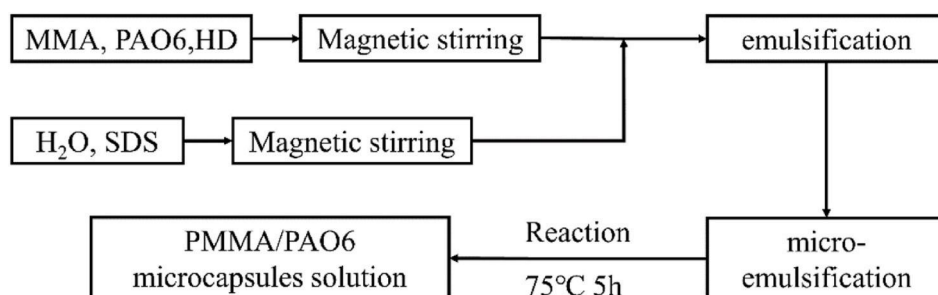


Fig. 1. PMMA/PAO6 microcapsule preparation scheme.

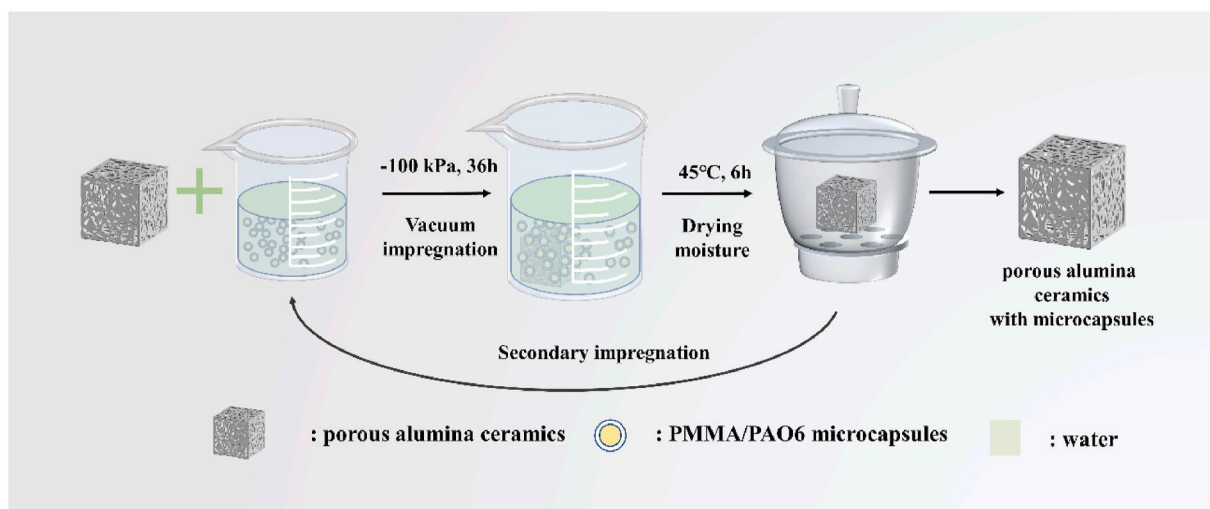


Fig. 2. Schematic diagram of the preparation of the self-lubricating porous alumina ceramics.

thoroughly with alcohol prior to each test. Raw porous alumina ceramics were used as the control group. Reciprocating friction stroke was 4 mm, the sliding speed was 16 mm/s, and the test loads were 3 N and 5 N.

### 3. Results and discussion

The prepared PMMA/PAO6 microcapsules were regular spheres with smooth surfaces, and PAO6 was tightly wrapped. Next, by adjusting the concentration of HD and SDS, the microcapsules with a particle size of 200–400 nm were obtained, as shown in Fig. 3 (b). As a result, the monomer dispersibility of the capsule solution was better, but it was

easy to form agglomerates after drying. The morphology after agglomeration is shown in Fig. 3 (c). The shell thickness of the PMMA/PAO6 microcapsules obtained from the TEM analysis of is shown in Fig. 3 (d).

As illustrated in Fig. 4(a), the porous alumina ceramics have a pore size of 3–5 μm. The porosity of porous alumina ceramics was calculated to be 41.55% measured by the Archimedes drainage method. As shown in Fig. 4(b), the adhered capsules can be observed on the surface of porous alumina ceramic with PMMA/PAO6 microcapsules. These microcapsules showed good dispersion at the smooth surfaces of porous alumina, many capsules can be seen in this area. Agglomerated capsules could be seen on the uneven surfaces of the porous alumina ceramics. It was because recesses provided conditions for the accumulation of

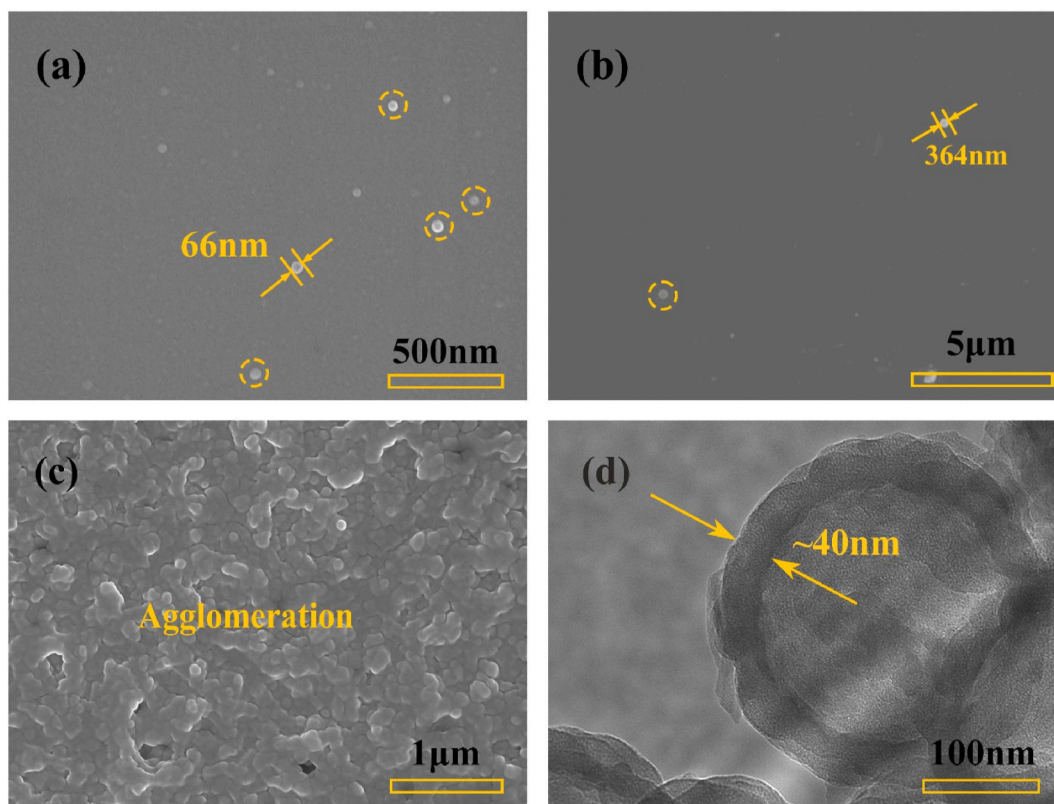


Fig. 3. (a) and (b) SEM images of PMMA/PAO6 microcapsules, (c) SEM image of PMMA/PAO6 microcapsules agglomeration, (d) TEM image of PMMA/PAO6 microcapsules.

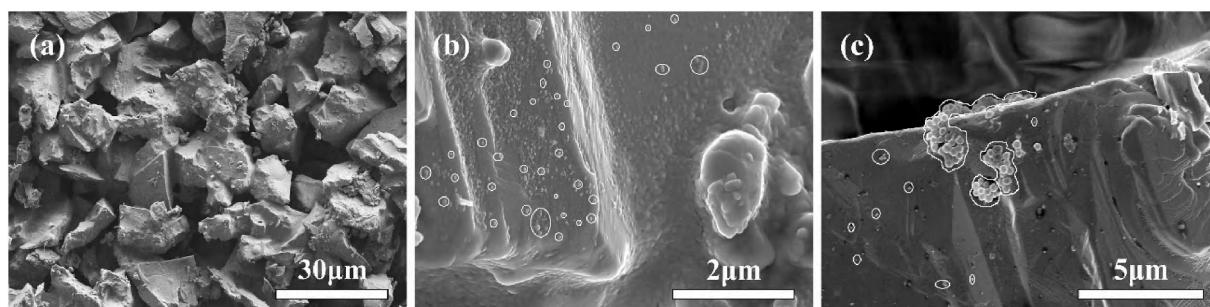


Fig. 4. (a) SEM images of porous alumina ceramics; SEM micrographs of (b) surface morphology, and (c) cross-section of porous alumina ceramics with microcapsules.

capsules, which leads more capsules reunited after drying. For the sake of observing whether PMMA/PAO6 microcapsules successfully permeate into porous alumina ceramics, SEM was taken to observe the cross-sectional morphology of porous alumina ceramics with microcapsules. As indicated in Fig. 4 (c), PMMA/PAO6 microcapsules could be observed, and these microcapsules were distributed individually or aggregated on the porous alumina ceramic matrix.

The XRD patterns of the porous alumina ceramics and porous alumina ceramics with PMMA/PAO6 microcapsules were compared in Fig. 5. The characteristic peaks of all samples were consistent with the standard alumina card. The intensity of all characteristic peaks of porous alumina ceramics with microcapsules was reduced. The results indicated that the structure of porous alumina ceramics was not destroyed during the process of vacuum impregnation, and the decrease of peak intensity proved that the PMMA/PAO6 microcapsules were distributed on porous ceramics.

In order to better understand the distribution of microcapsules in the porous alumina ceramic matrix, the cross-section was observed in detail by SEM. Fig. 6 presented the SEM cross-sectional image of the porous alumina ceramic with PMMA/PAO6 microcapsules. As shown in Fig. 6 (a), four areas were selected from top to bottom on the cross-section image with a total length of 5910  $\mu\text{m}$  for observation. In the four selected areas, the microcapsules adhering to the porous ceramic substrate could be seen. The distances from the four selected areas to the upper surface of the porous alumina ceramic are 1472  $\mu\text{m}$ , 2919  $\mu\text{m}$ , 4270  $\mu\text{m}$  and 5181  $\mu\text{m}$ . As the distance from the porous ceramic surface increases, the quantity of PMMA/PAO6 microcapsules gradually decreases. Many single and agglomerated microcapsules can be clearly

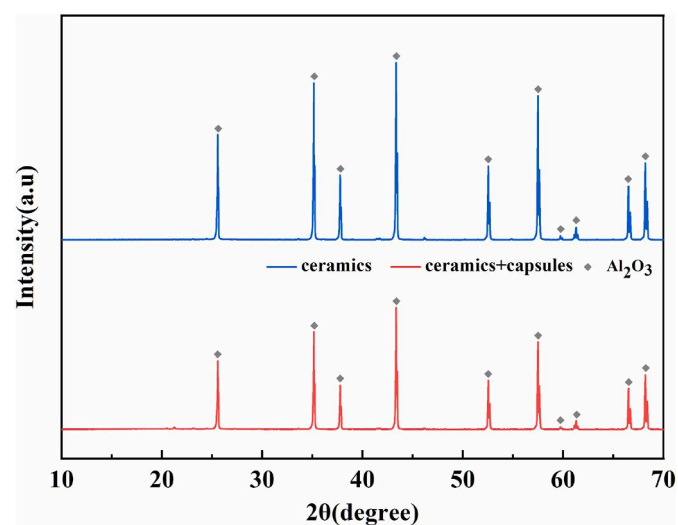


Fig. 5. XRD pattern of the porous alumina ceramics and the porous alumina ceramics with PMMA/PAO microcapsules.

seen in the porous ceramics as showcased in Fig. 6 (b2) and (e2). In the areas of Fig. 6 (c2) and Fig. 6 (d2), the microcapsules are relatively few. However, it was also apparent that many monodisperse capsules were uniformly distributed on the porous ceramic substrate. Agglomerated microcapsules could be seen at the junction of the porous ceramic particles. The EDS results in Fig. 7 was the element mapping of the porous alumina ceramics with PMMA/PAO6 microcapsules cross section.

The tribological performances of original ceramics, porous alumina ceramics with PMMA/PAO6 microcapsules were evaluated using the UMT3 tester. The lubricating properties of the porous alumina ceramics with PMMA/PAO microcapsules under different loads were studied. As illustrated in Fig. 8 (a), the porous alumina ceramics with PMMA/PAO6 microcapsules under 3 N and 5 N both showed low and stable COF, while the original ceramics showed the high COF. When the load increased from 3 N to 5 N, the COF changed drastically. The lubrication performance of the porous ceramics with the microcapsules was further studied, as shown in Fig. 8 (c). Under the load of 5 N, within a test period of 7200 s, the porous alumina ceramics with the PMMA/PAO6 microcapsules could obtain a lower COF, and it remained stable over time. The above results showed that the porous alumina ceramics with PMMA/PAO6 microcapsules had good self-lubricating properties. The results showed that the filling of PMMA/PAO6 microcapsules in porous ceramics could produce excellent lubricating properties. As shown in Fig. 8 (d), the lowest COF and wear rate of the porous alumina ceramic were 0.196 and  $96.74 \times 10^{-6} \text{ mm}^3/\text{N}\cdot\text{m}$ , which were only 20% and 0.17% of the original alumina porous ceramic (lowest COF: 0.962, wear rate:  $5611.49 \times 10^{-6} \text{ mm}^3/\text{N}\cdot\text{m}$ ). In order to explore the influence of porous ceramic pore size and capsule size on lubrication performance, the same way was used to process porous ceramics with self-lubricating properties whose pore sizes were around 200–400 nm. The only dissimilarity was that the microcapsule solution with a particle size of 60–70 nm was used for both dipping. Tribological experiments were carried out on the processed samples with pore diameters of 200–400 nm, as shown in Fig. 8 (b). The COF was not significantly different from the samples with pore diameters of 3–5  $\mu\text{m}$ . However, the addition of microcapsules also reduced the COF of porous ceramics in the range of 200–400 nm pore size. It showed that compared with changing the pore size, the addition of capsules had a greater impact on the lubricating performance of porous alumina ceramics.

As can be seen from Fig. 9 (a), the surface morphologies of the worn surface were examined using the surface profilometer. The width and depth of wear scars of porous alumina ceramics without PMMA/PAO6 capsule were wider and deeper. It also suggested that porous alumina ceramics without PMMA/PAO6 microcapsules were more likely to be worn. As shown in Fig. 9 (b), the energy spectrum analysis of the wear scars on the surface of porous alumina ceramics was performed. Elements of Al, O, and C existed in the non-wear region as shown in spectrum 2. Al and O are the main elements in porous alumina ceramics, and C was the main element in PMMA/PAO6 microcapsules. While in spectrum 1, in addition to Al, O, and C elements, the worn area also existed Zr element. It demonstrated that during the friction process, the

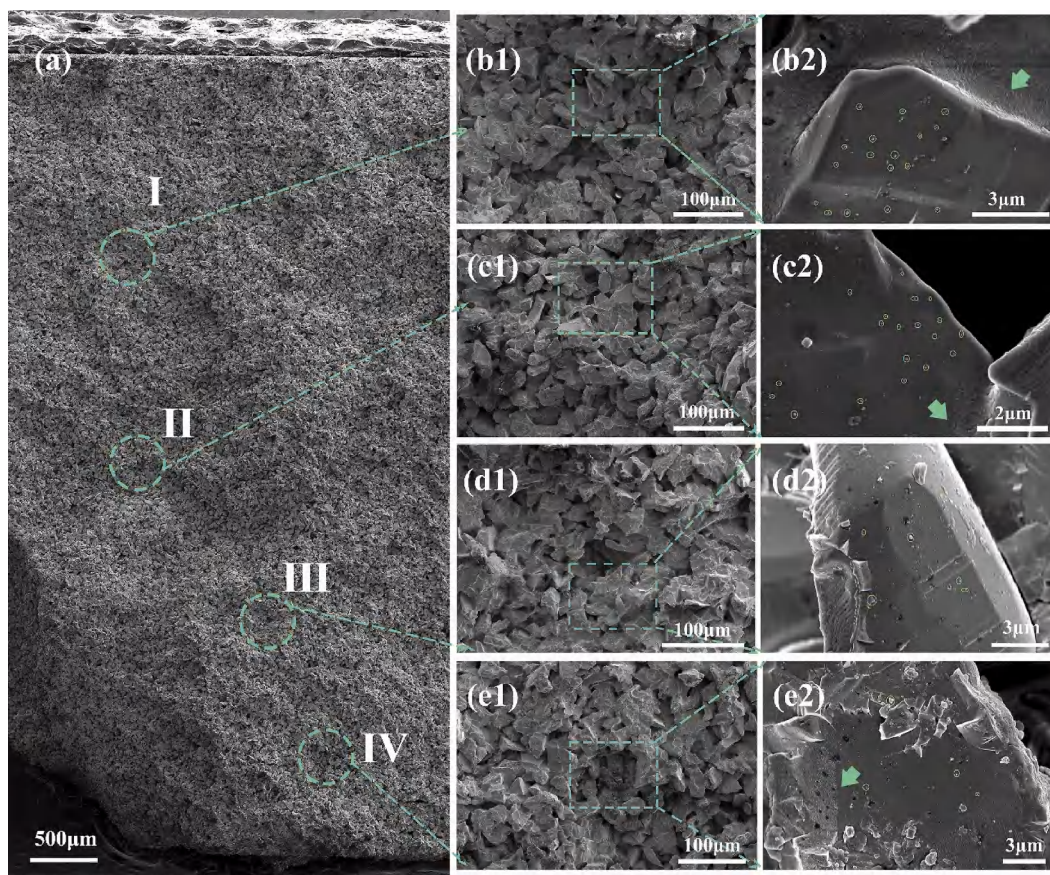


Fig. 6. SEM images of porous alumina ceramics with PMMA/PAO6 microcapsules (a) cross-section; (b1) and (b2) magnified SEM images of region I in Fig. 6(a); (c1) and (c2) magnified SEM images of region II in Fig. 6(a); (d1) and (d2) magnified SEM images of region III in Fig. 6(a); (e1) and (e2) magnified SEM images of region IV in Fig. 6(a). The agglomerated microcapsules were indicated by green arrows. (For interpretation of the references to colour in this figure legend, the reader is referred to the Web version of this article.)

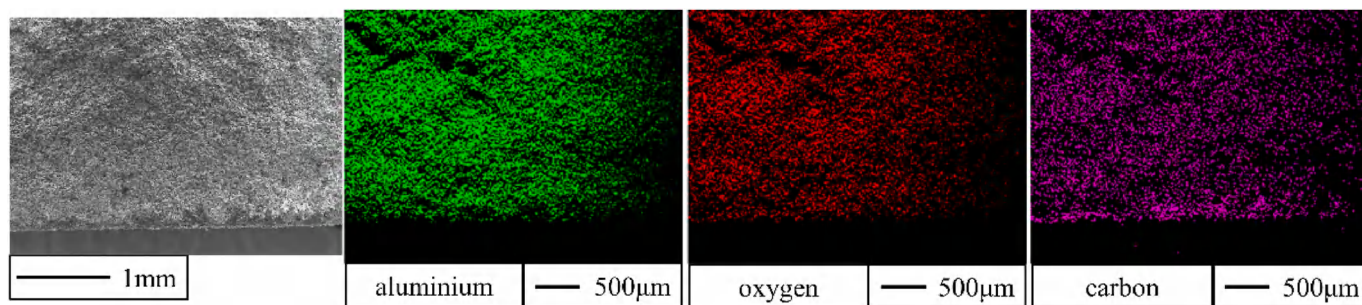


Fig. 7. Elemental diagram of porous alumina ceramic cross section.

Zr element in the grinding wheel was transferred to form wear debris and glued to the surface of porous alumina ceramics.

The lubrication mechanism of porous alumina ceramic with PMMA/PAO6 microcapsules was primarily due to the boundary lubricant film formed on a wear surface. As illustrated by Fig. 10 (c), PMMA/PAO6 microcapsules adhered to porous alumina ceramics were damaged during friction, and PAO6 lubricating oil was released [37]. The PAO6 lubricates the friction surface and prevents direct contact between the ZrO grinding ball and the porous alumina ceramic matrix. The wear debris generated in the friction process were also entered into the holes on the surface of porous ceramics. In the wear process, the microcapsule on the porous alumina ceramics surface was damaged first, and the PAO6 oil inside was released to play a lubricating effect, forming a stable film on the surface of the substrate. As the wear further occurs,

microcapsules deep in the porous ceramics were broken, and the oil inside was released to provide continuous and stable lubrication. As the wear time increases, more PAO6 oil was released. Therefore, low friction coefficient and wear rate were maintained.

#### 4. Conclusion

The PMMA/PAO6 microcapsules with two different particle sizes were prepared by microemulsion polymerization. Self-lubricating porous alumina ceramics were fabricated by impregnation vacuum the microcapsules into the porous ceramic substrate. For the tribology testing, the porous alumina ceramics with microcapsules showed outstanding self-lubrication property. As a result, a lower COF and wear rate were obtained, which were 0.196 and  $96.74 \times 10^{-6} \text{ mm}^3/\text{N}\cdot\text{m}$ ,

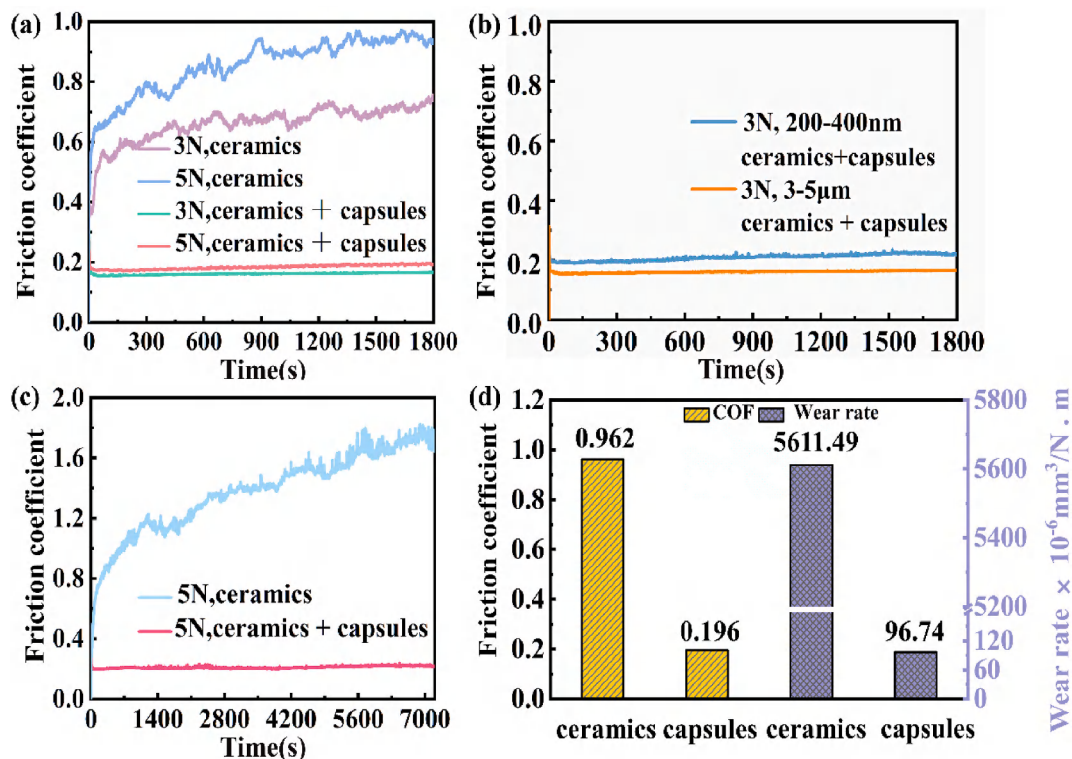


Fig. 8. (a) and (c) coefficient of frictions of the porous alumina ceramics and the porous alumina ceramics with microcapsules at different loads (pore size: 3–5 µm); (b) coefficient of frictions of the self-lubricating porous alumina ceramics with different pore size; (d) the wear rates of the samples (pore size: 3–5 µm).

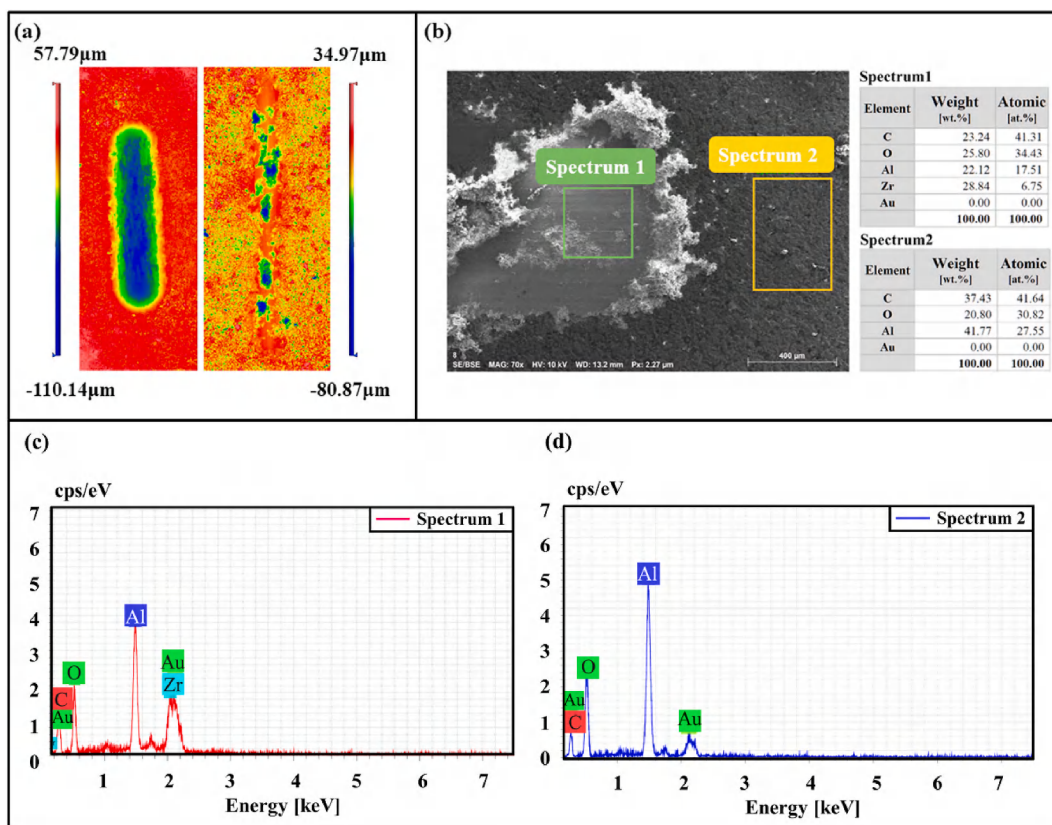


Fig. 9. (a) Surface morphologies of the worn surfaces of the samples (the porous alumina ceramics on the left side and the porous alumina ceramics with microcapsules on the right); (b), (c) and (d) the EDS of the porous alumina ceramics with microcapsules (spectrum1: the worn surface; spectrum2: the unworn surfaces).

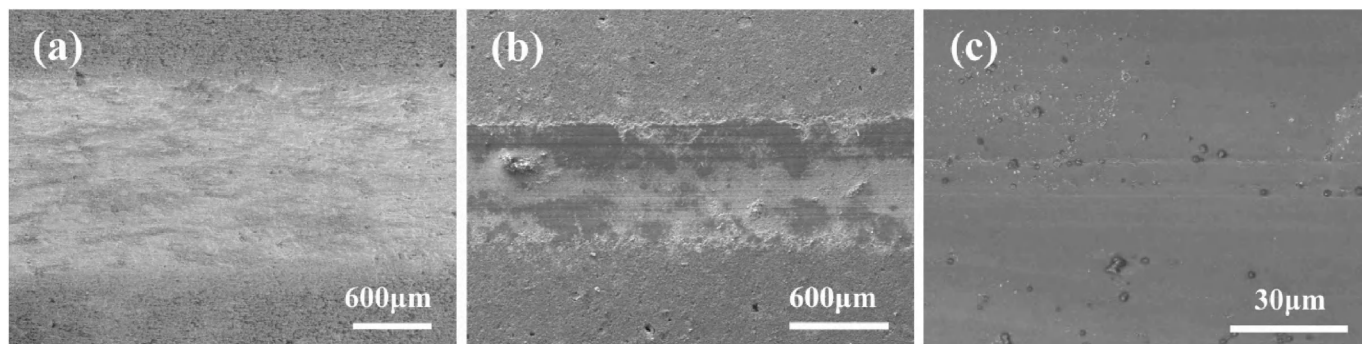


Fig. 10. High-magnification SEM images of the wear scars of (a) porous alumina ceramics, (b) and (c) self-lubricating porous alumina ceramics.

respectively. Besides, the effect of pore size on the lubricating efficiency of porous ceramics was also investigated, and studies have shown that the presence of microcapsules has more impact than the size of porous ceramics. During the friction process, the PAO oil released from the microcapsules formed a boundary lubrication film. This prevented direct contact between the two sliding surfaces, which reduced the coefficient of friction and the rate of wear.

#### Declaration of competing interest

The authors declare that they have no known competing financial interests or personal relationships that could have appeared to influence the work reported in this paper.

#### Acknowledgments

This work was supported by the National Natural Science Foundation of China (Grant No. 51822505, 51775044, 51811530014), the Pre Research Program in National 13th Five-Year Plan (Grant No.61409230603).

#### References

- [1] T.E. Steyer, Shaping the future of ceramics for aerospace applications, *Int. J. Appl. Ceram. Technol.* 10 (2013) 389–394, <https://doi.org/10.1111/ijac.12069>.
- [2] V.T. Rathod, J.S. Kumar, A. Jain, Polymer and ceramic nanocomposites for aerospace applications, *Appl. Nanosci.* 7 (2017) 519–548, <https://doi.org/10.1007/s13204-017-0592-9>.
- [3] P. Diaz-Rodríguez, M. López-Álvarez, J. Serra, P. González, M. Landín, Current stage of marine ceramic grafts for 3D bone tissue regeneration, *Mar. Drugs* 17 (2019) 1–16, <https://doi.org/10.3390/md17080471>.
- [4] X. Li, Y. Gao, S. Wei, Q. Yang, Tribological behaviors of B4C-hBN ceramic composites used as pins or discs coupled with B4C ceramic under dry sliding condition, *Ceram. Int.* 43 (2017) 1578–1583, <https://doi.org/10.1016/j.ceramint.2016.10.136>.
- [5] X.M. Yao, X.J. Wang, X.J. Liu, Z.M. Chen, Z.R. Huang, Friction-wear properties and mechanism of hard facing pairs of SiC and WC, *Wuji Cailiao Xuebao/Journal Inorg. Mater.* 34 (2019) 673–678, <https://doi.org/10.15541/jim20180435>.
- [6] M.R. Akbarpour, S. Alipour, A. Safarzadeh, H.S. Kim, Wear and friction behavior of self-lubricating hybrid Cu-(SiC + x CNT) composites, *Compos. B Eng.* 158 (2019) 92–101, <https://doi.org/10.1016/j.compositesb.2018.09.039>.
- [7] W. Zhang, S. Yamashita, T. Kumazawa, F. Ozeki, H. Hyuga, H. Kita, Effect of nanorelief structure formed in situ on tribological properties of ceramics in dry sliding, *Ceram. Int.* 45 (2019) 13818–13824, <https://doi.org/10.1016/j.ceramint.2019.04.078>.
- [8] K. Sang, Z. Lü, Z. Jin, A study of the SiC-L composite ceramics for self-lubrication, *Wear* 253 (2002) 1188–1193, [https://doi.org/10.1016/S0043-1648\(02\)00250-8](https://doi.org/10.1016/S0043-1648(02)00250-8).
- [9] A. Salam, G. Xie, D. Guo, W. Xu, Fabrication and tribological behavior of self-lubricating composite impregnated with synthesized inorganic hollow fullerene-like MoS<sub>2</sub>, *Compos. B Eng.* 200 (2020) 108284, <https://doi.org/10.1016/j.compositesb.2020.108284>.
- [10] J. Llorente, C. Ramírez, M. Belmonte, High graphene fillers content for improving the tribological performance of silicon nitride-based ceramics, *Wear* 430 (431) (2019) 183–190, <https://doi.org/10.1016/j.wear.2019.05.004>.
- [11] D. Wei, Q. Meng, D. Jia, Mechanical and tribological properties of hot-pressed h-BN/Si<sub>3</sub>N<sub>4</sub> ceramic composites, *Ceram. Int.* 32 (2006) 549–554, <https://doi.org/10.1016/j.ceramint.2005.04.010>.
- [12] V.I. Kulik, A.S. Nilov, A.P. Garshin, V.V. Savich, A.A. Dmitrovich, D.I. Saroka, Study of tribological properties of composite materials with a silicon carbide matrix, *Refract. Ind. Ceram.* 53 (2012) 259–268, <https://doi.org/10.1007/s11148-012-9504-4>.
- [13] W. Chen, D. Zhang, Z. Lv, H. Li, Self-lubricating mechanisms via the in situ formed tribo-film of sintered ceramics with hBN addition in a high humidity environment, *Int. J. Refract. Metals Hard Mater.* 66 (2017) 163–173, <https://doi.org/10.1016/j.ijrmhm.2017.03.014>.
- [14] K. Sang, Z. Jin, Unlubricated friction of reaction-sintered silicon carbide and its composite with nickel, *Wear* 246 (2000) 34–39, [https://doi.org/10.1016/S0043-1648\(00\)00352-5](https://doi.org/10.1016/S0043-1648(00)00352-5).
- [15] W. Tong, X. Song, C. Gao, Layer-by-layer assembly of microcapsules and their biomedical applications, *Chem. Soc. Rev.* 41 (2012) 6103–6124, <https://doi.org/10.1039/c2cs35088b>.
- [16] K. Chen, S. Zhou, S. Yang, L. Wu, Fabrication of all-water-based self-repairing superhydrophobic coatings based on UV-responsive microcapsules, *Adv. Funct. Mater.* 25 (2015) 1035–1041, <https://doi.org/10.1002/adfm.201403496>.
- [17] X. Wang, C. Zhang, K. Wang, Y. Huang, Z. Chen, Highly efficient photothermal conversion capric acid phase change microcapsule: silicon carbide modified melamine urea formaldehyde, *J. Colloid Interface Sci.* 582 (2021) 30–40, <https://doi.org/10.1016/j.jcis.2020.08.014>.
- [18] W. Luo, D. Sun, S. Chen, L. Shanmugam, Y. Xiang, J. Yang, Robust microcapsules with durable superhydrophobicity and superoleophilicity for efficient oil-water separation, *ACS Appl. Mater. Interfaces* 12 (2020) 57547–57559, <https://doi.org/10.1021/acami.0c15455>.
- [19] T. Bollhorst, K. Rezwani, M. Maas, Colloidal capsules: nano- and microcapsules with colloidal particle shells, *Chem. Soc. Rev.* 46 (2017) 2091–2126, <https://doi.org/10.1039/c6cs00632a>.
- [20] Y.B. Chong, D. Sun, X. Zhang, C.Y. Yue, J. Yang, Robust multifunctional microcapsules with antibacterial and anticorrosion features, *Chem. Eng. J.* 372 (2019) 496–508, <https://doi.org/10.1016/j.cej.2019.04.139>.
- [21] S.H. Hu, R.H. Fang, Y.W. Chen, B.J. Liao, I.W. Chen, S.Y. Chen, Photoresponsive protein-graphene-protein hybrid capsules with dual targeted heat-triggered drug delivery approach for enhanced tumor therapy, *Adv. Funct. Mater.* 24 (2014) 4144–4155, <https://doi.org/10.1002/adfm.201400080>.
- [22] D. Liu, Q. Shi, S. Jin, Y. Shao, J. Huang, Self-assembled core-shell structured organic nanofibers fabricated by single-nozzle electrospinning for highly sensitive ammonia sensors, *Info 1* (2019) 525–532, <https://doi.org/10.1002/inf2.12036>.
- [23] M.R. Kim, Z. Xu, G. Chen, D. Ma, Semiconductor and metallic core-shell nanostructures: synthesis and applications in solar cells and catalysis, *Chem. Eur. J.* 20 (2014) 11256–11275, <https://doi.org/10.1002/chem.201402277>.
- [24] L. Zhang, G. Xie, S. Wu, S. Peng, X. Zhang, D. Guo, S. Wen, J. Luo, Ultralow friction polymer composites incorporated with monodispersed oil microcapsules, *Friction* 9 (2021) 29–40, <https://doi.org/10.1007/s40544-019-0312-4>.
- [25] H. Gong, Y. Song, G.L. Li, G. Xie, J. Luo, A highly tough and ultralow friction resin nanocomposite with crosslinkable polymer-encapsulated nanoparticles, *Compos. B Eng.* 197 (2020), <https://doi.org/10.1016/j.compositesb.2020.108157>.
- [26] H. Sertchook, D. Avnir, Submicron silica/polystyrene composite particles prepared by a one-step sol-gel process, *Chem. Mater.* 15 (2003) 1690–1694, <https://doi.org/10.1021/cm020980h>.
- [27] S. Peng, L. Zhang, G. Xie, Y. Guo, L. Si, J. Luo, Friction and wear behavior of PTFE coatings modified with poly (methyl methacrylate), *Compos. B Eng.* 172 (2019) 316–322, <https://doi.org/10.1016/j.compositesb.2019.04.047>.
- [28] A. Sari, C. Alkan, A. Biçer, Thermal energy storage characteristics of micro-nanoencapsulated heneicosane and octacosane with poly(methylmethacrylate) shell, *J. Microencapsul.* 33 (2016) 221–228, <https://doi.org/10.3109/02652048.2016.1144820>.
- [29] H. Li, S. Li, Z. Li, Y. Zhu, H. Wang, Polysulfone/SiO<sub>2</sub> hybrid shell microcapsules synthesized by the combination of pickering emulsification and the solvent evaporation technique and their application in self-lubricating composites, *Langmuir* 33 (2017) 14149–14155, <https://doi.org/10.1021/acs.langmuir.7b03370>.
- [30] M. Li, H. Wang, D. Liu, R. Wang, Y. Zhu, Tribological and mechanical properties of self-lubrication epoxy composites filled with activated carbon particles containing lubricating oil, *RSC Adv.* 6 (2016) 52596–52603, <https://doi.org/10.1039/c6ra07698j>.
- [31] H. Li, Y. Cui, Z. Li, Y. Zhu, H. Wang, Fabrication of microcapsules containing dual-functional tung oil and properties suitable for self-healing and self-lubricating

- coatings, *Prog. Org. Coating* 115 (2018) 164–171, <https://doi.org/10.1016/j.porgcoat.2017.11.019>.
- [32] F. Wu, J. Li, H. Quan, J. Han, X. Liu, X. Zhang, J. Yang, Y. Xiang, Robust polyurea/poly(urea–formaldehyde) hybrid microcapsules decorated with Al<sub>2</sub>O<sub>3</sub> nano-shell for improved self-healing performance, *Appl. Surf. Sci.* 542 (2021) 148561, <https://doi.org/10.1016/j.apsusc.2020.148561>.
- [33] A. Imani, H. Zhang, M. Owais, J. Zhao, P. Chu, J. Yang, Z. Zhang, Wear and friction of epoxy based nanocomposites with silica nanoparticles and wax-containing microcapsules, *Compos. Part A Appl. Sci. Manuf.* 107 (2018) 607–615, <https://doi.org/10.1016/j.compositesa.2018.01.033>.
- [34] X. He, D. Wu, R. Jia, X. Liu, Z. Huang, D. Wang, C. Zhao, Z. Hui, Novel polyurethane elastomer modified by hybrid shell nano-/microcapsules for unique self-lubricating behavior, *Ind. Eng. Chem. Res.* 59 (2020) 22123–22131, <https://doi.org/10.1021/acs.iecr.0c04586>.
- [35] G. Wu, C. Xu, G. Xiao, M. Yi, Z. Chen, H. Chen, An advanced self-lubricating ceramic composite with the addition of core-shell structured h-BN@Ni powders, *Int. J. Refract. Metals Hard Mater.* 72 (2018) 276–285, <https://doi.org/10.1016/j.jrmhm.2017.12.038>.
- [36] J. Guo, Q. Pan, C. Huang, Y. Zhao, X. Ovyang, Y. Huo, S. Duan, The role of surfactant and costabilizer in controlling size of manocapsules containing TEGDMA in miniemulsion, *J. Wuhan Univ. Technol.-Materials Sci. Ed.* 24 (2009) 1004–1006, <https://doi.org/10.1007/s11595-009-7004-2>.
- [37] X. Zhang, P. Wang, D. Sun, X. Li, J. An, T.X. Yu, E.H. Yang, J. Yang, Dynamic plastic deformation and failure mechanisms of individual microcapsule and its polymeric composites, *J. Mech. Phys. Solid.* 139 (2020), <https://doi.org/10.1016/j.jmps.2020.103933>.